ELSEVIER

PII: S0032-3861(97)10321-4

Polymer Vol. 39 No. 16, pp. 3713–3718, 1998

0032-3861/98/$19.00+0.00

Stress relaxation of a main-chain, smectic, polydomain liquid crystalline elastomer

C. Ortiz†, C. K. Ober* and E. J. Kramer‡
Cornell University, Department of Materials Science and Engineering and The Materials Science Center, Bard Hall, Ithaca, NY 14850, USA
(Received 2 October 1997; accepted 16 November 1997)

It has recently been shown that liquid crystalline elastomers (LCEs) exhibit bulk macroscopic orientation or a 'polydomain-to-monodomain' transition when stretched in uniaxial tension (see for example review articles by: Gleim, W. and Finkelmann, H., *Side-Chain Liquid Crystal Polymers*, ed. C. B. McArdle. Blackie and Sons Ltd., 1989, p. 287; Zentel, R., *Agnew Chem. Adv. Mater.*, 1989, *101*(10), 1437; Barclay, G. G. and Ober, C. K., *Prog. Polym. Sci.*, 1993, *18*, 899–945). In order to investigate this phenomenon further, single-step stress relaxation experiments were performed in uniaxial tension on a polydomain, smectic LCE at variable strains relative to the polydomain-to-monodomain transition. It was found that the smectic LCE exhibited a large amount of stress relaxation and could be described at intermediate times ($\approx$ 7–3000 s) by a stretched exponential function with a relatively fast characteristic relaxation time ($\approx$ 60 s), regardless of the magnitude of the strain. One possible origin of this phenomenon is that the local smectic LC order is transiently disrupted during initial deformation and reorientation of the LC domains. The free energy penalty for this disruption may provide a driving force for reversion back to the original (undeformed) state of order and, correspondingly, a large amount of local chain relaxation. It was also found that the stress relaxation data were divided into two regimes. At low strains (prior to the polydomain-to-monodomain transition) the data exhibited a final relaxed modulus of $E_f = 1.8$ MPa. Samples stretched to larger strains (greater than the polydomain-to-monodomain transition) were shifted to lower values with $E_f = 0.7$ MPa.

(Keywords: liquid crystalline elastomer; stress relaxation; polydomain-to-monodomain transition)

INTRODUCTION

Recently, there has been much interest in a new class of loosely cross-linked network materials called liquid crystalline elastomers (LCEs)[1]. The combination of the entropic elasticity of a flexible polymer backbone with the orientational ordering of the rigid-rod, LC molecules leads to many unusual phenomena, including spontaneous shape changes at LC phase transitions[2,3], strain-induced orientational transitions leading to new LC morphologies[4], distinctive dynamic mechanical properties[5] and 'soft elasticity'[6]. The structure and properties of the LCE investigated in this study are reviewed extensively elsewhere[7,8]. To summarize, the system has a 'main-chain' network structure (i.e. the LC molecules are incorporated directly into the polymer backbone), smectic-type local ordering, a glass transition temperature T_g of 36°C and an LC-to-isotropic ('clearing') transition temperature T_i of 98°C. On a larger scale, the LCE exhibits a macroscopically disordered, polydomain, Schlieren texture (when viewed under the polarizing optical microscope) with an average LC domain size ($\approx$ average distance between disclinations) of 2–3 μm.

Most experimental work to date has concentrated on 'side-chain' LCEs in which the LC molecules are attached to the polymer backbone via a flexible spacer group. One of the most remarkable characteristics of LCEs is the ability to undergo a polydomain-to-monodomain transition; i.e. stress-induced macroscopic orientation of the directors within the LC domains to form a 'liquid single crystal elastomer'. This phenomenon is a well-known universal characteristic of both main-chain and side-chain, nematic and smectic LCEs[7–25], regardless of chemical structure. An LCE deformed in uniaxial tension exhibits a nominal stress *versus* nominal strain curve with three regimes and a unique relationship between orientation parameter, *S*, and nominal stress[8,13–15,25]. The nature of each of these three regions is described in more detail in *Figure 1*. There is much speculation on exactly how the polydomain-to-monodomain transition takes place[26–30]. When deformed in tension, the LC domains elongate and rotate their local director orientations along the tensile axis[8]. For a main-chain, smectic LCE, the orientation and strain are permanently 'frozen in' upon the removal of stress by the oriented layered structure[8], suggesting minimal chain relaxation. The purpose of this research is to investigate this phenomenon further through single-step stress relaxation tests at various strains relative to the polydomain-to-monodomain transition in a main-chain, smectic LCE. We feel that these experiments will provide a more concrete basis for theoretical comparison and also give clues as to the driving forces behind the polydomain-to-monodomain transition.

EXPERIMENTAL

Materials

The liquid crystalline epoxy monomer used in this study, the diglycidyl ether of 4,4′-dihydroxy-α-methylstilbene

* To whom correspondence should be addressed
† Present address: Department of Polymer Chemistry, University of Groningen, Nijenborgh 4, 9747 AG Groningen, The Netherlands
‡ Present address: Materials Department, University of Santa Barbara, Santa Barbara, CA 93106-5050, USA

(DGDHMS), was synthesized and characterized as described previously[8]. The monomer was mechanically mixed with decanedioic (sebacic) acid (SA, 98% purity, Aldrich Chemical Co.) in a molar ratio of 1:1[7]. The finely ground mixture was placed in a glass mould which had been previously coated in a 3 mM solution of octadecyltrichlorosilane in 80%/20% hexadecane/carbon tetrachloride to provide a non-reactive, non-stick coating and then cured in the isotropic phase of the mixture at 180°C for 1.5 h. Characterization of the networks is described elsewhere[8] and was achieved using Fourier transform infrared spectroscopy (Galaxy Series 2020 FTIR), nuclear magnetic resonance (Varian XL-200 ^{1}H NMR), wide-angle X-ray diffraction (WAXD, Scintag generator), differential scanning calorimetry (Perkin-Elmer DSC-7) and polarizing optical microscopy (POM, Nikon Optiphot-2).

For comparison, experiments were also performed on cross-linked polyisoprene samples prepared in the following manner. Polyisoprene (84 wt%), sulfur (3.9 wt%), 'Altax' accelerator (3.9 wt%) and 'Age-Rite' (inhibits high-temperature degradation, 7.7 wt%) were masticated and cured at 175°C under pressure for 15 min. The glass transition temperature of the network was approximately −60°C.

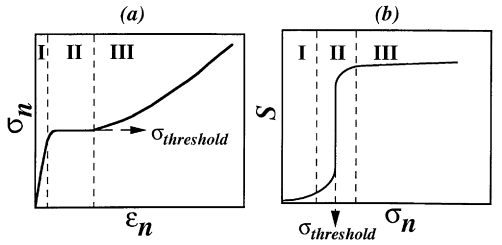

Region I:	At small strains, the polydomain elastomer deforms linear elastically with a typical rubber modulus, corresponding to a small nonlinear increase in the orientation of the material with nominal stress.
Region II:	At intermediate strains, a polydomain-to-monodomain transition takes place where the sample is converted from turbid to optically transparent or translucent. During this time, the LC domains elongate and the local director orientations rotate along the stress axis[8]. The transparency of the sample indicates that thermal fluctuations of the director are suppressed strongly by coupling to the network[6]. The phase transition leads to a plateau in the stress versus strain curve and corresponds to a dramatic increase in S at a critical threshold stress, $\sigma_{threshold}$. The drop in apparent elastic modulus has been attributed to inhomogeneous deformation[8].
Region III:	At large strains, the apparent modulus increases again (although to a different value) and only a small amount of additional orientation is achieved.

Figure 1 Schematic of (a) nominal stress *versus* nominal strain curve and (b) orientation parameter *versus* nominal stress of a polydomain LCE

Mechanical experiments

Uniaxial tension experiments were performed on 0.1 in × 0.04 in × 0.4 in samples using an Instron (Model 1125) mechanical testing machine equipped with a CCF A20 lb load cell at a displacement rate 0.2 in min^{-1}. Temperature control was achieved with an environmental chamber and temperature controller (Applied Test Systems MTF 310). The DGDHMS/SA elastomer was tested at ≈ 55°C (i.e. within the smectic phase) and the polyisoprene rubber was tested at room temperature. Force, f, versus displacement, δ, data were taken and converted into nominal stress, σ_n, versus nominal strain, ε_n. For the smectic LCE (*Figure 2a*), three regimes were observed due to a polydomain-to-monodomain transition as described in the Introduction. The polyisoprene rubber exhibited large-strain, non-linear, elastic behaviour typical of an isotropic, amorphous elastomer (*Figure 2b*). The large increase in stress which occurs at high extensions is due to the finite extensibility of the network strands and macroscopic orientation of the network. The tensile rubbery modulus, E_R, obtained was used to estimate the degree of cross-linking with reasonable accuracy using equation (1) from classical rubber elasticity theory[31]:

$$< M_x > = \frac{3\rho RT}{E_R} \quad (1)$$

where $< M_x >$ is the average molecular weight between cross-links, ρ is the density of the network, T is the absolute temperature (K) and R is the universal gas constant. For the polyisoprene rubber the modulus was found to be $E_R \approx$ 1.5 MPa, giving a value of $< M_x > \approx$ 7700 g mol^{-1}. For the DGDHMS/SA elastomer (within the isotropic phase, $T \approx$ 105°C), the modulus was found to be $E_R \approx$ 0.5 MPa, giving a value of $< M_x > \approx$ 22 900 g mol^{-1} (≈ 50 monomers).

Stress relaxation experiments were performed in uniaxial tension with the same experimental apparatus described above for the uniaxial tension tests. The samples were extended up to the appropriate amount of initial strain, ε_o, the cross-head movement stopped to maintain the strain constant, and the force decay measured as a function of time, t. The force was subsequently converted into nominal stress. The experiments on the DGDHMS/SA elastomer were conducted at ≈ 55°C (i.e. within the smectic phase) and the polyisoprene rubber was tested at room temperature. The smectic LCT was extended up to ε_o = 0.15, 0.45, 1.16, and 2.61 and the polyisoprene rubber was extended up to ε_o = 1.75 (shown schematically in *Figure 2*).

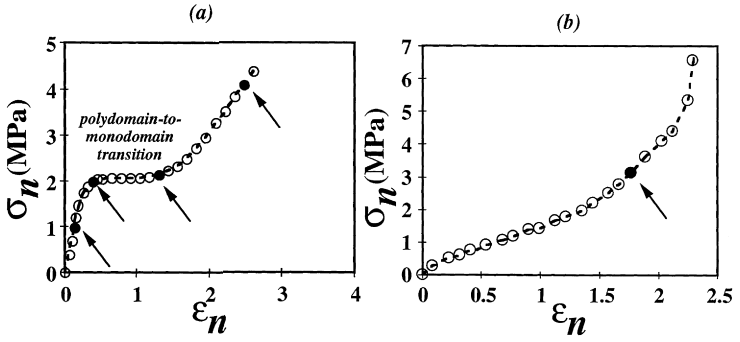

Figure 2 Nominal stress versus nominal strain curves for the (a) DGDHMS/SA polydomain smectic LCE and (b) polyisoprene rubber showing schematically the initial strains, ε_o, used for the stress relaxation experiments (●)

Data analysis

The stress relaxation curves were fitted to a single stretched exponential function as described by a modification of the Kohlrausch–Williams–Watt (KWW) equation[32]:

$$\sigma_n(t) = (\sigma_{max} - \sigma_{min}) \exp(-t/\tau)^{\beta} + \sigma_{min} \quad (2)$$

where t is the experimental time, σ_{max} is the instantaneous (unrelaxed) nominal stress at $t = 0$, σ_{min} is the long-time (relaxed) stress at $t = \infty$, and τ is the characteristic relaxation time. The value of the parameter β in equation (2) is a measure of the narrowness of the distribution and is approximately 0.5 for flexible, isotropic polymers. The KWW equation is successful in describing a wide variety of relaxation phenomena in polymeric and non-polymeric solids including dielectric relaxation[33], hypersonic relaxation[34] and dynamic bulk relaxation[35]. Other distribution functions such as a two-component cumulative log–normal distribution[36,37] have been employed to describe more thermorheologically complex materials.

The time-dependent relaxation modulus, E_R, and corresponding form of the KWW equation are given as follows:

$$E_R(t) = \sigma_n(t)/\varepsilon_o \quad (3)$$

$$E_R(t) = (E_o - E_f) \exp(-t/\tau)^{\beta} + E_f \quad (4)$$

where $E_o = E_R(t = 0)$ is the instantaneous (unrelaxed) modulus, $E_f = E_R(t = t_f) \approx E_R(t = t_\infty)$ is the long-time (relaxed) modulus, and t_f is the final time recorded in the stress relaxation experiment. If $E_R(t)$ is independent of the magnitude of the strain, ε_o, the material is defined as linear viscoelastic (LVE), typically true for strains, $\varepsilon_o < 1\%$[38]. For larger strains in the non-LVE regime, it has been shown that in many cases the stress relaxation curves can be shifted by horizontal time shifts to produce a master curve which predicts the relaxation behaviour at long times[39,40], analogous to time–temperature-superposition[38]. The relaxation strength, Δ, can be defined according to equation (5):

$$\Delta = (E_o - E_f)/E_f \quad (5)$$

In order to estimate β and τ from the experimental data, equation (4) was rearranged to obtain equation (6):

$$\ln \ln[(1/R(t)] = \beta \ln(t/\tau) \quad (6)$$

where $R(t)$ is the 'relaxation function' which is equal to $(E(t) - E_f)/(E_o - E_f)$. The data are more convenient to analyse in this form since a plot of the left-hand side of equation (6) *versus* the $\ln(t)$ is linear with a slope $= \beta$ and a y-intercept of $-\beta \ln \tau$.

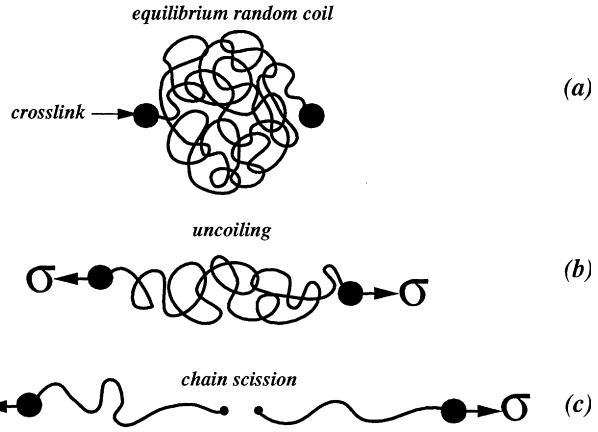

Figure 3 Possible molecular mechanisms for stress relaxation in non-LC, amorphous, isotropic elastomers: (a) equilibrium random coil configuration of a single network strand ($\sigma = 0$); (b) rearrangement (uncoiling) of polymer chains ($\sigma > 0$) at short times; (c) chain scission of covalent bonds at long times and elevated temperatures

RESULTS AND DISCUSSION

Polyisoprene

The viscoelastic phenomenon of stress relaxation has been well-documented for many years in elastomers[41–43], amorphous, glassy polymers[37,39,40,44–46], polymer fibres[38] and non-polymeric glass-forming liquids[35,47]. The stress relaxation process observed in these experiments is primarily due to conformational changes: the uncoiling/disentangling of polymer chains between network junctions in order that they may obtain a lowered free energy state (*Figure 3*). This rearrangement involves cooperative motions between neighbouring segments and secondary dipole–dipole and van der Waals interactions between polymer chains, as well as the rotation of carbon–carbon, covalent backbone bonds. *Figure 4* plots the stress relaxation curve, $\sigma_n(t)$, for the polyisoprene rubber at short (400 s) and long (6000 s) times. The strength of the relaxation was found to be rather small, $\Delta = 0.19$, and the final relaxation modulus was found to be $E_f = 1.3$ MPa. It has been shown[41,42] that a much larger decay of stress occurs at elevated temperatures (≈150°C) for natural and synthetic rubbers and longer times (2–100 h) due to chemical degradation (i.e. chain scission of carbon–carbon covalent bonds).

Figure 4 is replotted as $\ln[\ln(1/R(t))]$ versus $\ln(t)$ in *Figure 5*. At intermediate times (≈ 7–2900 s), the data

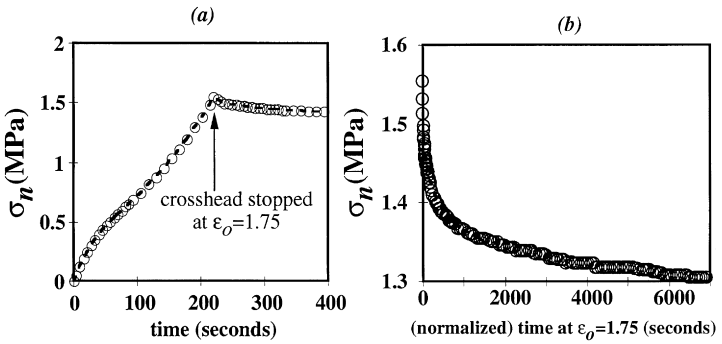

Figure 4 Stress relaxation curves of nominal stress *versus* time for polyisoprene rubber (a) on loading and at short times and (b) at long times (the time is normalized by setting $t = 0$ when the cross-head was stopped, corresponding to σ_{max})

could be fitted well to the stretched exponential function with a characteristic relaxation time of $\tau \approx 415$ s and $\beta \approx 0.42$. At short and long times, the data deviate rapidly and non-linearly from the empirical fit, being overestimated at short times and underestimated at long times.

Smectic LCE

Figures 6 and *7* are examples of typical stress relaxation curves, $\sigma_n(t)$, for the DGDHMS/SA smectic LCE at short (200 s) and long (3000 s) times before ($\varepsilon_o = 0.45$) and after ($\varepsilon_o = 2.61$) the polydomain-to-monodomain transition. All of the curves appeared to reach a steady stress value by the end of the experiment. *Figure 8* compares the time-dependent relaxation moduli of the DGDHMS/SA smectic LCE samples stretched to different initial strains: $\varepsilon_o = 0.15$, 0.45, 1.16, and 2.61. From these plots, it is immediately observed that the strength of relaxation, $\Delta \approx 2.33$, is much larger than that of the polyisoprene rubber, $\Delta \approx 0.19$, and also approximately constant for all strains. The data corresponding to initial strains prior to the polydomain-to-monodomain transition superimpose with a final relaxation modulus of $E_f = 1.8$ MPa. The curves after the transition also nearly superimpose, but to a lower value of $E_f = 0.7$ MPa. This result indicates that the relaxation behaviour is affected by the degree of macroscopic orientation and is clearly different for the polydomain and monodomain structures.

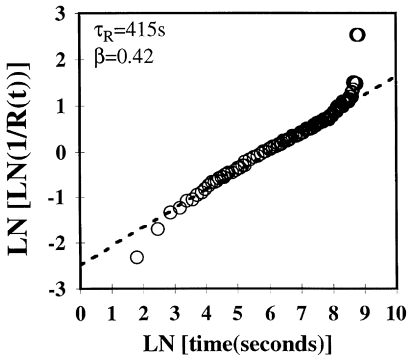

Figure 5 Double logarithmic plot of the relaxation function, ln[ln(1/*R*(*t*))], *versus* time, ln(*t*), for polyisoprene rubber with stretched exponential fit (– – –), i.e. equation (6)

Figures 6 and *7* are replotted as ln[ln(1/*R*(*t*))] *versus* ln(*t*) as *Figures 9* and *10* respectively. The same general trend is observed as seen for the polyisoprene rubber, i.e. non-linear deviations from the stretched exponential function at short and long times. No significant differences in the empirical fit for β (≈ 0.40) and τ (≈ 79 s) were observed for the samples stretched to different strains.

A surprising result from these experiments is the large amount of stress relaxation and fast characteristic relaxation time found for the smectic LCE compared to the polyisoprene, given the fact that these materials also exhibit a large mechanical hysteresis. In other words, even though the strain and orientation (i.e. the aligned LC domain structure) are 'frozen' in at all strains when the stress is removed, the sample still undergoes significant stress relaxation, suggesting that the origin of this relaxation takes place on a localized size scale of less than a single LC domain ($\sim\mu$m). The large stress relaxation may be partially due to the fact that the material is very close to T_g ($T - T_g \approx 20$°C) and has a lower cross-link density than the polyisoprene rubber, giving a higher mobility to the

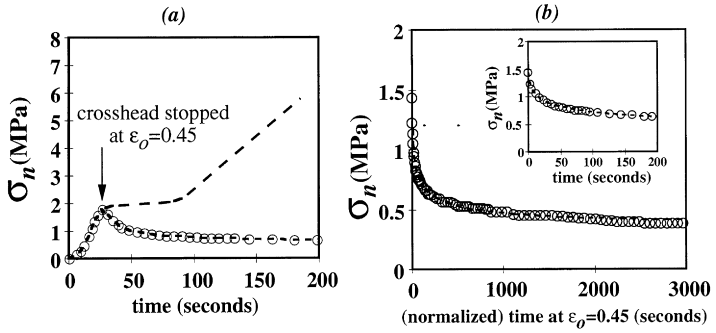

Figure 6 Stress relaxation curves of nominal stress *versus* time for the DGDHMS/SA smectic LCE before the polydomain-to-monodomain transition (a) on loading and at short times and (b) at long times (the time is normalized by setting $t = 0$ when the cross-head was stopped, corresponding to σ_{max})

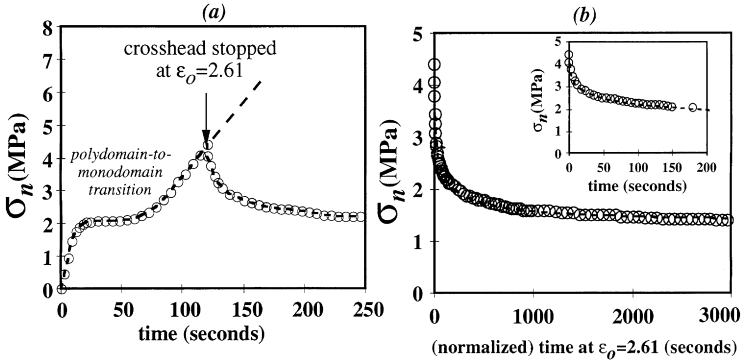

Figure 7 Stress relaxation curves of nominal stress *versus* time for the DGDHMS/SA smectic LCE after the polydomain-to-monodomain transition (a) on loading and at short times and (b) at long times (the time is normalized by setting $t = 0$ when the cross-head was stopped, corresponding to σ_{max})

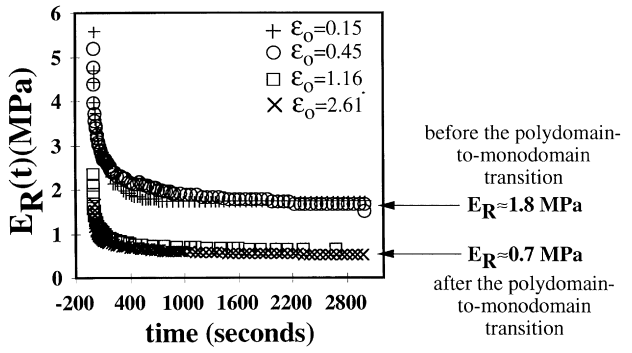

Figure 8 Plots of the relaxation moduli *versus* time for the DGDHMS/SA smectic LCE

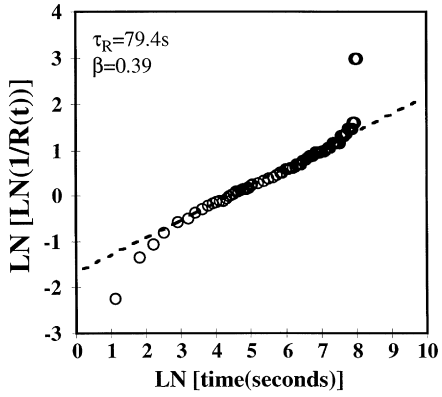

Figure 9 Double logarithmic plot of the relaxation function, ln[ln(1/*R*(*t*))], versus time, ln(*t*), for the DGDHMS/SA smectic LCE before the polydomain-to-monodomain transition, $\varepsilon_o = 0.45$, with stretched exponential fit (– – –), i.e. equation (6)

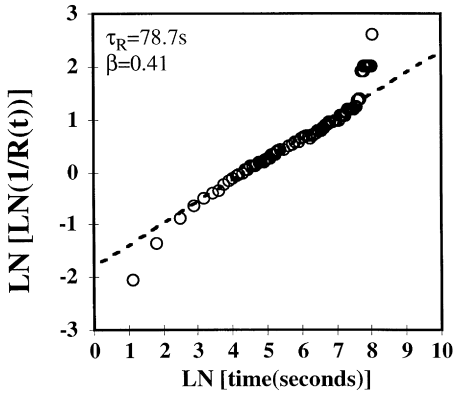

Figure 10 Double logarithmic plot of the relaxation function, ln[ln(1/*R*(*t*))], versus time, ln(*t*), for the DGDHMS/SA smectic LCE before the polydomain-to-monodomain transition, $\varepsilon_o = 2.61$, with stretched exponential fit (– – –), i.e. equation (6)

network strands. It is also possible that the locally ordered, smectic LC structure facilitates local chain relaxation and may contribute to the stress plateau in the nominal stress *versus* nominal strain curve. During deformation and reorientation of the LC domains, the smectic layers may contract and become disordered (for domains unfavourably oriented) or expand and become more ordered (for domains favourably oriented). The free energy penalty for this disruption may provide a driving force for reversion back to the original (undeformed) smectic structure at the new increased value of macroscopic orientation.

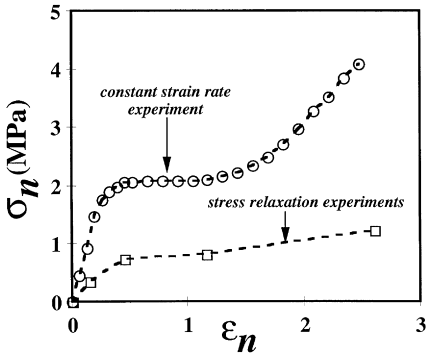

Figure 11 Nominal stress *versus* nominal strain curves for the DGDHMS/SA polydomain, smectic LCE: constant strain rate experiment (○) compared to data from the stress relaxation experiments, i.e. final stress measured ($t = t_f$) (□)

A plot of the nominal stress *versus* nominal strain curve obtained from the stress relaxation experiments (i.e. $\sigma(t_f)$ *versus* ε_o) is compared to that obtained from a constant strain rate experiment (i.e. $\sigma(t_{initial})$ *versus* ε_o) in *Figure 11*. The stress relaxation data are obviously shifted down, but still maintain a qualitatively similar shape.

CONCLUSIONS

Single-step stress relaxation experiments were performed in uniaxial tension on an epoxide-based, main-chain, smectic LCE at variable strains relative to the polydomain-to-monodomain transition and fitted to a stretched exponential function. It was found that this material exhibited a large amount of stress relaxation: approximately an order of magnitude greater than amorphous, isotropic polyisoprene rubber. The relaxation moduli of the smectic LCE could be described by a stretched exponential function with a single, relatively fast characteristic relaxation time ($\tau \approx 60$ s), regardless of the magnitude of the strain. One possible origin of this phenomenon is that the local smectic LC order is transiently disrupted during deformation and reorientation of the LC domains. The free energy penalty for this disruption may provide a driving force for reversion back to the original, undeformed state of order, and hence facilitate local chain relaxation. Even though τ and β were found to be approximately the same for all strains, the data were observed to be separated into two regimes. The samples stretched to low strains (prior to the polydomain-to-monodomain transition) were shifted to higher values compared to the samples stretched to larger strains (greater than the polydomain-to-monodomain transition). This division of the data suggests that the stress relaxation behaviour was influenced by the degree of macroscopic orientation.

ACKNOWLEDGEMENTS

The authors would like to acknowledge the following people who assisted in polymer synthesis: Jia Shiun-Lin, Audrey Robinson, Drs Yakhov Freidzon, Allen Gabor, Scott Clingman, Guo Ping Mao, Hilmar Koerner, and Michael Wagner. For technical consultation we would also like to thank Dr Hilmar Koerner, Atsushi Shiota and Maura Weathers (X-ray diffraction experiments and analysis), Margaret Rich (optical microscopy), Dr Jan Genzer (image analysis), John Hunt (SEM) and George Chevalier (mechanical testing). For many helpful discussions, we are

grateful to Drs Mark Warner and Eugene Terentjev. This research was sponsored by the National Consortium for Graduate Degrees for Minorities in Science and Engineering (GEM, Inc.), The Department of Education and the National Science Foundation.

REFERENCES

1. See for example review articles by: Gleim, W. and Finkelmann, H., *Side-Chain Liquid Crystal Polymers*, ed. C. B. McArdle. Blackie and Sons Ltd., 1989, p. 287; Zentel, R., *Agnew Chem. Adv. Mater*., 1989, *101*(10), 1437; Barclay, G. G. and Ober, C. K., *Prog. Polym. Sci.*, 1993, *18*, 899–945.
2. Mitchell, G. R., Davis, F. J. and Guo, W., *Phys. Rev. Lett.*, 1993, **71**, 2047.
3. Küpfer, J. and Finkelmann, H., *Makromol. Chem. Rapid Commun.*, 1991, **12**, 717.
4. Kundler, I. and Finkelmann, H., *Macromol. Chem. Rapid. Commun.*, 1995, **16**, 679–686.
5. Pakula, T. and Zentel, R., *Makromol. Chem.*, 1991, **192**, 2401.
6. See for example review article by: Warner, M. and Terentjev, E. M., *Prog. Polym. Sci.*, 1996, *21*, 853–891.
7. Giamberini, M., Amendola, E. and Carfagna, C., *Makromol. Rapid Commun.*, 1995, **16**, 97–105.
8. Ortiz, C., Wagner, M., Bhargava, N., Ober, C. K. and Kramer, E. J., *Macromolecules*, submitted for publication.
9. Hammerschmidt, K. and Finkelmann, H., *Makromol. Chem.*, 1989, **190**, 1089–1101.
10. Finkelmann, H., Kock, H.-J., Gleim, W. and Rehage, G., *Makromol. Chem. Rapid Commun.*, 1984, **5**, 287–293.
11. Mitchell, G. R., Coulter, M., Davis, F. J. and Guo, W., *J. Phys. II France*, 1992, **2**, 1121–1132.
12. Zentel, R. and Benalia, M., *Makromol. Chem.*, 1987, **188**, 665–674.
13. Barnes, N. R., Davis, F. J. and Mitchell, G. R., *Mol. Cryst. Liq. Cryst.*, 1989, **168**, 13–25.
14. Davis, F. J., Gilbert, A., Mann, J. and Mitchell, G. R., *J. Polym. Sci., Part A: Polym Chem.*, 1990, **28**, 1455–1472.
15. Schätzle, J., Kaufhold, W. and Finkelmann, H., *Makromol. Chem.*, 1989, **190**, 3269–3284.
16. Kaufhold, W., Finkelmann, H. and Brand, H. R., *Makromol. Chem.*, 1989, **192**, 2555–2579.
17. Finkelmann, H. and Brand, H. R., *Trends in Polym. Sci.*, 1994, **2**(7), 222–226.
18. Brand, H. R., *Makromol. Chem. Rapid Commun.*, 1989, **10**, 57.
19. Meier, W. and Finkelmann, H., *Mater. Res. Soc. Bull.*, 1991, **16**(1), 29.
20. Zentel, R. and Reckert, G., *Makromol. Chem.*, 1986, **187**, 1915–1926.
21. Zentel, R., Schmidt, G. F., Meyer, J. and Benalia, M., *Liq. Cryst.*, 1987, **2**(5), 651–664.
22. Canessa, G., Reck, B., Reckert, G. and Zentel, R., *Makromol. Symp.*, 1986, **4**, 91–101.
23. Bualek, S., Kapitza, H., Meyer, J., Schmidt, G. F. and Zentel, R., *Mol. Cryst. Liq. Cryst.*, 1988, **155**, 47–56.
24. Barclay, G. G., McNamee, S. G., Ober, C. K., Papathomas, K. I. and Wang, D. W., *J. Polym. Sci.: Part A, Polym. Chem.*, 1992, **30**, 1845–1853.
25. Shiota, A., Cornell University, unpublished results, 1996.
26. Clarke, S. M., Nishikawa, E., Finkelmann, H. and Terentjev, E. M., submitted for publication.
27. Zhao, Y., *Polymer*, 1995, **36**, 2717–2724.
28. ten Bosch, A. and Varichon, L., *Macromol. Theory Simul.*, 1994, **3**, 533–542.
29. Terentjev, E. M., Proceedings of the NATO Advanced Research Workshop, Manipulation of Organization in Polymers using Tandem Molecular Interactions, Pisa, Italy, 29 May–2 June 1996.
30. Fridrikh, S. V. and Terentjev, E. M., in preparation.
31. Treloar, L. R. G., *The Physics of Rubber Elasticity*. Clarendon Press, Oxford, 1975.
32. Williams, G. and Watts, D. C., *Trans. Faraday Soc.*, 1971, **67**, 1323.
33. Matsuoka, S., *Relaxation Phenomenon in Polymers*. Hanser Press, 1985.
34. Patterson, G. D., *Macromolecules*, 1981, **14**, 84.
35. Johari, G. P., *J. Chem. Phys.*, 1973, **58**, 1966.
36. Wortmann, F. J. and Schultz, K. V., *Polymer*, 1995, **36**(12), 2363–2369.
37. Povolo, F., Schwartz, G. and Hermida, E. B., *J. Polym. Sci.: Part B, Polym. Phys.*, 1996, **34**, 1257–1267.
38. Ferry, J. D., *Viscoelastic Properties of Polymers*, 2nd edn. Wiley, NY, 1970.
39. Tieghi, G., Fallini, A. and Levi, M., *Polym. Commun.*, 1991, **32**(8), 245.
40. Tieghi, G., Levi, M., Fallini, A. and Danusso, F., *Polymer*, 1991, **32**, 39–43.
41. Tobolsky, A. V., Prettyman, I. B. and Dillon, J. H., *J. Appl. Physics*, 1944, **15**, 380.
42. Tobolsky, A. V., *Properties and Structure of Polymers*. Clarendon Press, Oxford, 1960, Chapter 5.
43. Björk, F. and Stenberg, B., *Polymer*, 1990, **31**, 1649.
44. Zhao, Y., Jasse, B. and Monnerie, L., *Polymer*, 1989, **30**, 1643.
45. Catsiff, E. and Tobolsky, A. V., *J. Colloid. Sci.*, 1955, **10**, 375.
46. Marin, G. and Graessley, W. W., *Rheol. Acta*, 1977, **16**, 527.
47. Angell, C. A. and Sichina, W., *Ann. N.Y. Acad. Sci.*, 1976, **279**, 53.